

Numerical investigation of entropy generation in unsteady MHD generalized Couette flow with convective cooling

O. Kigodi¹, M. H. Mkwizu¹, A X Matofali¹, M. A. Selemeni¹, N. Ainea¹, S. Khamis² and G. K. Karugila¹

¹Department of Mathematics, Informatics and Computational Sciences, Solomon Mahlangu College of Science and Education, Sokoine University of Agriculture, Morogoro-Tanzania

²The State University of Zanzibar, Department of Natural Science, Tanzania

Received: 25 November 2019, Accepted: 29 December 2019

Published online: 31 December 2019.

Abstract: This study aimed at making an investigation on entropy generation in unsteady MHD generalized couette flow with convective cooling. Specifically the study intended to; develop flow model for a case of nanofluid in a channel, determine the effect of different parameters on velocity, temperature and entropy generation and to determine the effect of magnetic field on the flow on an entropy generation. Also the study aim to come up with distinctively recommendation on dynamics of entropy generation, temperature variation and velocity profiles in unsteady MHD flow with convective cooling. Findings showed that an increase in nanoparticles and Reynolds number leads to increase in the velocity while pressure gradient, MHD and nanofluid fraction held constant. It is evidently that Alumina-water nanofluid tends to raise the velocity profile faster than Copper-water nanofluid. Also the results show that an increase in Eckert number causes the decrease in temperature profile. Further, it was noticed that Copper-water nanofluid tends to raise the temperature profile faster than Alumina-water nanofluid. More interestingly it was observed that the entropy generation rises as the result of increase in Eckert number. Also it is noticed that entropy generation rises in lower plate but when it comes closer the upper plate the entropy generation rate starts to fall as the result of increase in nanoparticles.

Keywords: Magneto hydrodynamic (MHD), Couette flow, nanofluids, entropy generation.

1 Introduction

The flow of electricity with nanofluids are now days much applicable referring to the industrial development in every part of the world, among of its applications includes of the following; geothermal reservoirs, nuclear reactor cooling, Magneto Hydrodynamic (MHD) marine propulsion, electronic packaging, microelectronic device operations, thermal insulation, and petroleum reservoirs.

According to (Trisaksri, 2007), Suspended nanoparticles in various base fluids can alter the fluid flow and heat transfer characteristics of the base fluids. These suspensions of nano sized particles in the base fluids are called nanofluids. Nanofluids are suspensions of nanoparticles in a base fluid, typically water. Materials used for nanoparticles and base fluids: Nanoparticle materials include: Oxide ceramics – Al_2O_3 , CuO Metal carbides – Sic Nitrides – AlN, SiN Metals – Al, Cu Non-metals – Graphite, carbon nanotubes Layered – Al + Al_2O_3 , Cu + C. The figure below shows the depicted picture of Nanoparticles and base fluids and the real mixture of normal particle into nanoparticles: Das, Jana and Chamkha (2015) investigated the entropy generation in a rotating Couette flow with suction/injection and they came up with the findings that; the entropy generation increases with an increase either rotation parameter or suction parameter or Brinkmann number or Prandtl number or group parameter. Rotations as well as suction/injection exert a significant

* Corresponding author e-mail: mkwizu@sua.ac.tz

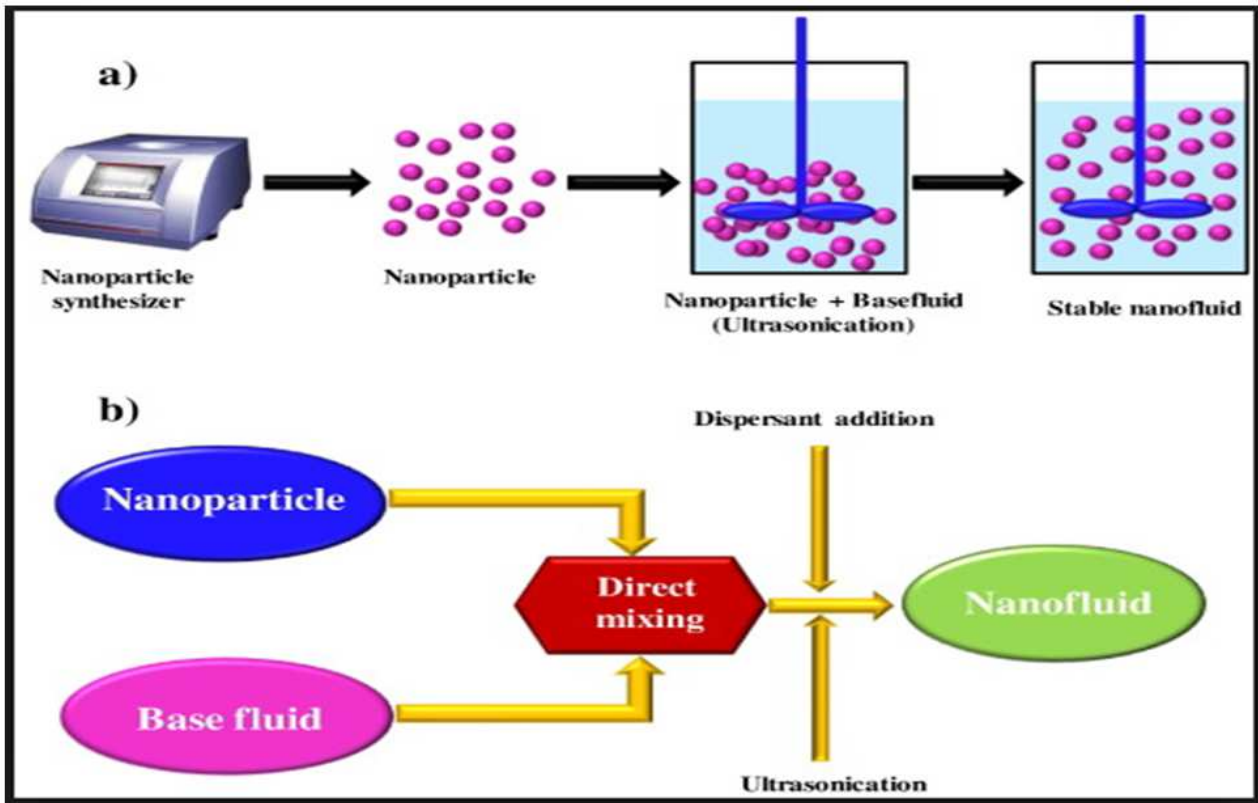


Fig. 1: Nanofluid- sciencedirect.com.

influence on the velocity and temperature distributions, which transitively affects the entropy generation within the channel. It is also found that magnitude of entropy generation due to fluid friction takes higher value for higher group parameter. Entropy minimization takes place when both plates are almost at the same temperature. When this same temperature value is higher, minimum value of entropy tends to take place at higher temperature.

Ali and Makinde (2015) made an investigation on modelling the effect of variable viscosity on unsteady Couette flow of Nanofluids with convective cooling, the result shows that While other parameter remain unchanged, the velocity profile increases with the increase of A or variable viscosity parameter β . Temperature decrease with the increase of β (increasing β decrease viscosity) or Bi with other parameters remain unchanged. Rising Ec cause temperature profile to rise while demonstrating little effect on both velocity and particle volume distribution profile, variation of Schmidt number Sc shows significant effect on the nanoparticle volume distribution profile before the system reached steady state, and demonstrates no effect at all. A combined similarity-numerical solution of MHD boundary layer slip flow of non-Newtonian power-law nanofluids along a moving radiating vertical flat plate explored by Nur Husna, Jashim Uddin and AhmadIzani (2014). It was discovered that the dimensionless velocity, the temperature and the nanoparticles volume fraction decrease with n . The dimensionless velocity decreases while the temperature and the nanoparticles volume fraction increase with M . The dimensionless velocity decreases while the temperature and the nanoparticles volume fraction increase with a . The dimensionless nanoparticles volume fraction decreases with Le . The dimensionless temperature increases with R . The friction factor increases with the increase of M , whilst it is decreased with a . The heat transfer rate increases with n and Pr decreases with a , Nb , Nt . The nanoparticles volume fraction rate increases with Le and n and decreases with a . Mkwizu and Makinde (2015) come up with the investigation about entropy generation in a

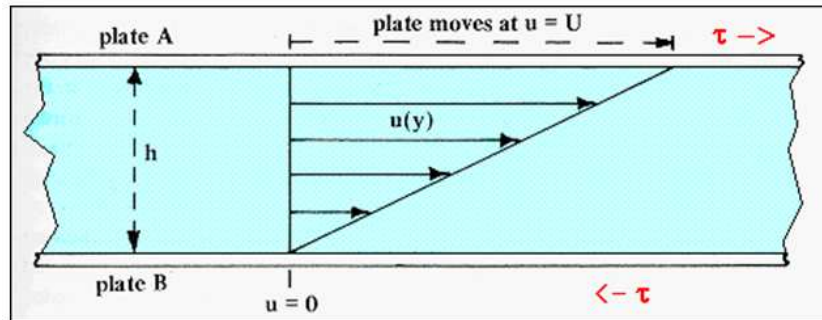


Fig. 2: Newtonian Law of Shear Viscosity to Entropy Density rate-engineeringtoolbox.com.

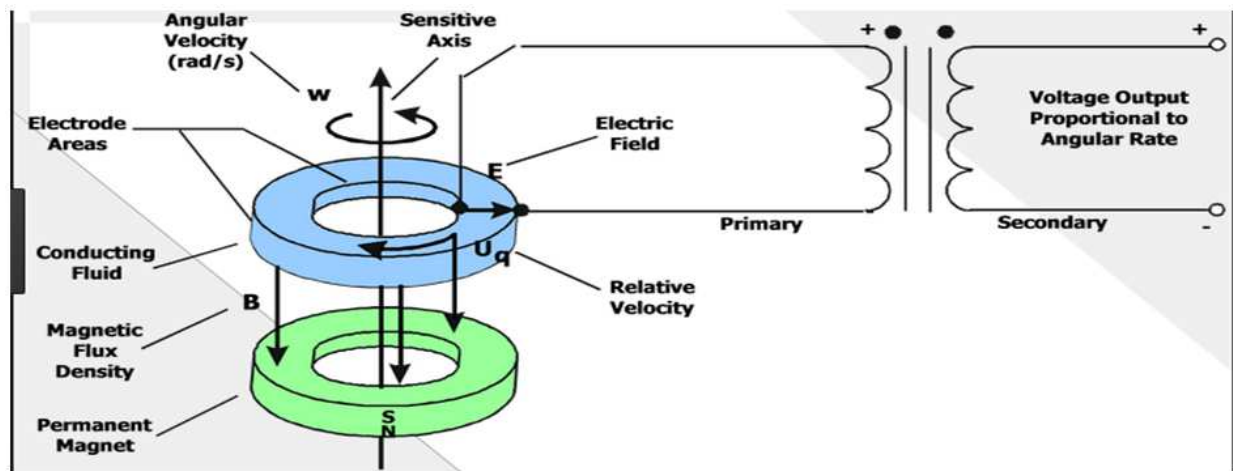


Fig. 3: MHD Technology- atacorp.com.

variable viscosity channel flow of nanofluids with convective cooling and the results were as follows; the nanofluids velocity and temperature profiles increase with increasing t , β , Ec , but decreases with increasing Bi , nanoparticle concentration increases along the centreline region and decreases near the walls, with an increase in t , β , Ec , Nt . However, an increase in Bi or Nb causes a decrease in nanoparticle concentration along the centreline region, whereas the concentration increases near the walls, Also they have observed that the skin friction increases with t , β , Ec , Nt and A , but decreases with Ec and Nt . The Nusselt number increases with t , Ec , Bi and β . According to investigations done by Alfaryjat et al., (2016) the result shows that, the overall entropy generation rate and entropy generation number are obtained by integrating the volumetric rate components over the entire heat sink. The results indicated that entropy generation decreases with increases of the Reynolds number, also decreasing the heat flux led to decreasing entropy generation.

According to the investigations done by Lyimo and Mkwizu (2016) the result shows that Alumina-water nanofluids have higher temperature value compare to copper-water nanofluids. Also they have observed that Alumina-water nanofluids have a tendency to reach steady state in a velocity profile early than Copper-water nanofluids and at the certain time both will reach steady state. Furthermore, they came up with the observed fact that an entropy generation is directly proportional to pressure gradient (A), Eckert number (Ec), Prandtl number (Pr). Entropy generation is inversely proportional to Reynolds number (Re) and nanoparticles volume fraction (ϕ), however it was observed that when

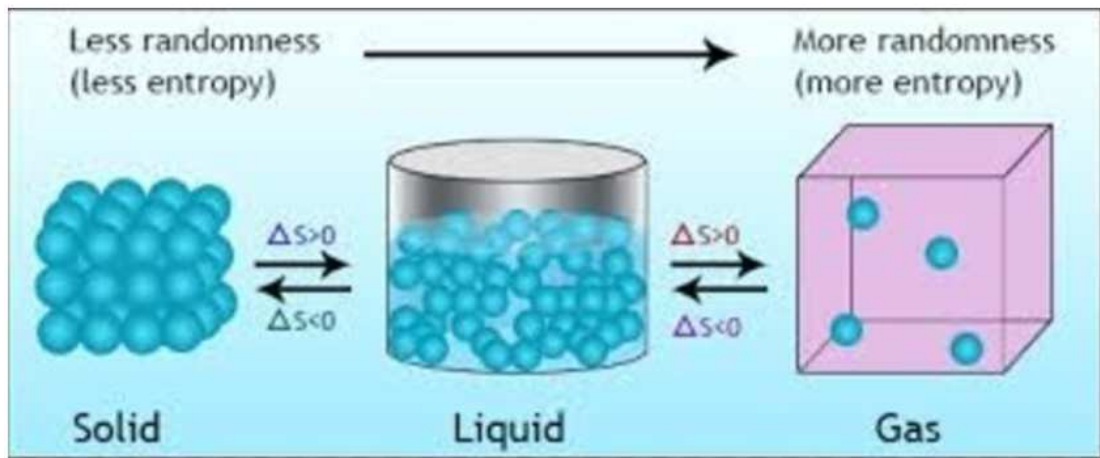


Fig. 4: Entropy randomness- crypto.stackexchange.com.

$\phi = 0$ entropy generation rate is so faster than when ϕ not equal to zero value.

Mkwizu, Makinde and Nkansah-Gyekye (2015) have investigated that an increase in nanoparticles volume fraction and Reynolds number causes a decrease in the velocity profile. Meanwhile nanofluid velocity profile increases with an increase in pressure gradient. Also the temperature profile increases with an increase in the nanoparticles volume fraction, slip parameter and Eckert number. But a decrease in temperature profile is noticed with an increase in Biot number. They also came up with the results that skin friction increases with an increase in nanoparticles volume fraction, slip parameter and Reynolds number. But decrease with an increase in pressure gradient. The same results are obtained for the Nusselt number and the rise in an entropy generation rate is observed with an increase in nanoparticles volume fraction and slip parameter.

Makinde and Eegunjobi (2013) made investigation in analysis of inherent irreversibility in a variable viscosity magneto-hydrodynamic (MHD) generalized couette flow with permeable walls. They found that the optimal design and the efficient performance of a flow system or a thermally designed system can be improved by choosing the appropriate values of the physical parameters. And this was because of there are effect towards the upper and lower moving plates. Also they observed that An increase in Ec , Pr , and Bi increases the velocity profiles, while an increase in Ha and Bi_0 decreases the velocity profile along channel center line region.

Chinyoka and Makinde (2013) came up with the investigation of entropy generation in unsteady MHD generalized Couette flow with variable electrical conductivity. The results shows that due to the nature of the source terms, the fluid velocity and temperature will each decrease (resp., increase) with a corresponding increase in the parameters that decrease/increase the magnitudes of the source terms. They have also demonstrated computationally that parameters which increase the entropy generation rate will correspondingly decrease the Bejan number and vice versa. Also the observation revealed that, as the flow profiles vary in shape from linear to “parabolic” in response to varying parameter values, the velocity or temperature gradients correspondingly change in magnitude leading to noticeable effects in the entropy generation rates and Bejan numbers.

According to Baskaya, Komurgoz and Ozkol (2017), an increase in magnetic field density suppresses the flow field significantly, and these effects get stronger as the volume fraction of nanoparticles in nanofluids increases. The velocity

and temperature increases as the inclination of the channel rises but this tendency diminishes with larger magnetic field intensity or volume fraction of nanofluids. Also they revealed that the velocity decreases with an increase in volume fraction of nanoparticles due to the fact that when magnetic field gets stronger, the volume fraction dependence of the velocity also increases and gets more dependent to temperature distribution. Further the results shows that, the entropy size decreases with increasing magnetic field angle for smaller values of channel inclination under the limitations that, for higher values of channel inclination, with an increase in magnetic field angle, the entropy generation first decreases and then increases. The minimum entropy generation is observed around when the magnetic field angle is perpendicular to the channel.

Kareem et al., (2017) made an investigation on entropy generation rate in unsteady buoyancy-driven hydro-magnetic couple stress fluid flow through a porous channel. They found that the entropy generation rate in the fluid model that has been studied largely depends on the internal forces between the fluid parcels. For example, as the couple stress parameter increases from zero, the electrically conducting fluid builds up more resistance against its flow rate, counted for the observed increase in the entropy generation rate with respect to the couple stress parameter. Also the result shows that an entropy generation trends found their cause to the internal phenomenon in the fluid though may be triggered by other forces such as the buoyancy and the Lorentz forces. In addition, it was observed that the presence of the Lorentz force in the fluid could be utilize to implement a speed control mechanism in the studied fluid system since increasing magnetic field in the fluid reduces velocity.

2 Mathematical models

Consider unsteady generalised Couette flow of viscous incompressible nanofluids containing Copper (Cu) and Alumina (Al_2O_3) as nanoparticles. It was assumed that the upper wall moves with uniform velocity u at time $t > 0$ and exchange heat with the ambient surrounding following the Newton’s law of cooling. It was further assumed that a magnetic field of uniform of strength B_0 act to the perpendicular to the plate. Take a Cartesian coordinate system (x, y) where x lies along the flow direction, y was the distance measured in the normal direction as depicted in figure 5 below:

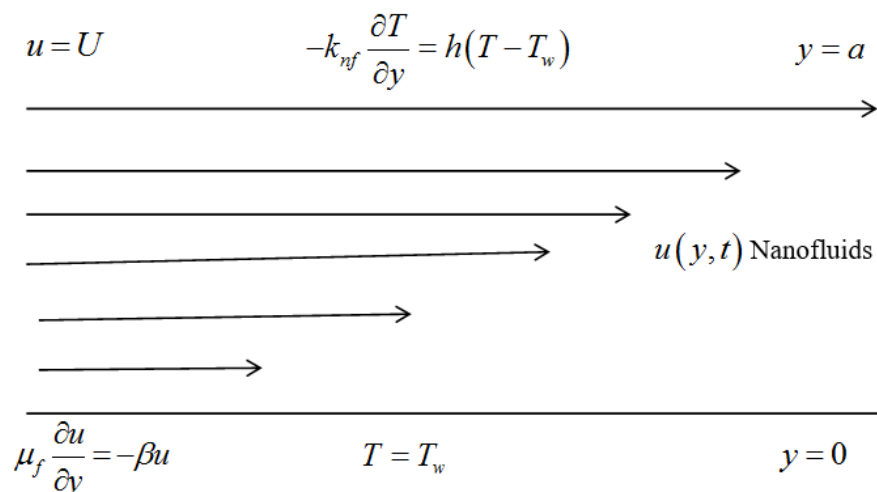


Fig. 5: Schematic diagram of the problem under consideration.

The Navier-Stokes continuity, nanofluids momentum and energy balance equations in one dimension under the Boussinesq approximation for the transient channel flow can be written as

$$\frac{\partial u}{\partial x} = 0 \quad (1)$$

$$\frac{\partial u}{\partial t} = -\frac{1}{\rho_{nf}} \frac{\partial P}{\partial x} + \frac{\mu_{nf}}{\rho_{nf}} \frac{\partial^2 u}{\partial y^2} - \frac{\sigma_w \beta_0}{\rho_f} \quad (2)$$

$$\frac{\partial T}{\partial t} = \alpha_{nf} \frac{\partial^2 T}{\partial y^2} + \frac{\alpha_{nf} \mu_{nf}}{k_{nf}} \left(\frac{\partial u}{\partial y} \right)^2 \quad (3)$$

where u is the nanofluid velocity in the x -direction, T is the temperature of the nanofluid, P is the nanofluid pressure, t is the time, a is the channel half width, T_w is the ambient temperature, μ_{nf} is the dynamic viscosity of the nanofluid, k_{nf} is the nanofluid thermal conductivity, ρ_{nf} is the density of the nanofluid, and α_{nf} is the thermal diffusivity of the nanofluid. The dynamic viscosity of nanofluid will be assumed to be temperature independent

(Abu-Nada 2008; Makinde 2012) as follows:

$$\mu_{nf} = \frac{\mu_f}{(1 - \phi)^{2.5}} \quad (4)$$

$$\rho_{nf} = (1 - \phi) \rho_f + \phi \rho_s \quad (5)$$

$$\alpha_{nf} = \frac{k_{nf}}{(\rho c_p)_{nf}} \quad (6)$$

$$\tau = \frac{(\rho c_p)_s}{(\rho c_p)_f} \quad (7)$$

$$\frac{k_{nf}}{k_f} = \frac{(k_s + 2k_f) - 2\phi(k_f - k_s)}{(k_s + 2k_f) + \phi(k_f - k_s)} \quad (8)$$

$$(\rho c_p)_{nf} = (1 - \phi) (\rho c_p)_f + \phi (\rho c_p)_s \quad (9)$$

The quantity of nanoparticles fraction will be represented by ϕ ($\phi = 0$ correspond to a regular fluid), ρ_f and ρ_s are the densities of the base fluid and the nanoparticle respectively, k_f and k_s are the thermal conductivities of the base fluid and the nanoparticles respectively where $(\rho c_p)_f$ is a heat capacitance of the base fluid and $(\rho c_p)_s$ is a heat capacitance of a nanoparticle .

Table below presents thermo-physical properties of water, copper and alumina at a given temperature. The initial conditions for solving Stoke Navier Equations and Newton's law of cooling will be given as;

$$\mu_f \frac{\partial u}{\partial x} (y, 0) = -\beta u (y, 0) \quad (10)$$

$$T (y, 0) = T_w \quad (11)$$

The boundary conditions for solving Stoke Navier Equations and Newton's law of cooling will be given as;

$$u (a, t) = U \quad (12)$$

Physical properties	Fluid phase (water)	Copper Cu	Alumina Al ₂ O ₃
c_p (J/kg K)	4179	385	765
ρ (kg/m ³)	997.1	8933	3970
k (W/m K)	0.613	401	40

Table 1: Thermophysical properties of the fluid phase (water) and nanoparticles

$$T(0, t) = T_w \tag{13}$$

$$\mu_f \frac{\partial u}{\partial x}(0, t) = -\beta u(0, t) \tag{14}$$

$$-k_{nf} \frac{\partial T}{\partial y}(a, t) = h(T(a, t) - T_w) \tag{15}$$

Introducing the dimensionless variables and parameters into Eqns (1) up to (16) as follows;

$$\left. \begin{aligned} \theta &= \frac{T-T_w}{T_w}, \quad W = \frac{u}{U}, \quad \bar{t} = \frac{tU}{a}, \quad v_f = \frac{\mu_f}{\rho_f}, \quad \bar{P} = \frac{Pa}{\mu_f U} \\ A &= -\frac{\partial \bar{P}}{\partial X}, \quad X = \frac{x}{a}, \quad \eta = \frac{y}{a}, \quad Pr = \frac{\mu_f c_{p_f}}{k_f}, \quad Ec = \frac{U^2}{c_{p_f} T_w} \\ \tau &= \frac{(\rho c_p)_s}{(\rho c_p)_f}, \quad m = \frac{(k_s + 2k_f) + \phi(k_f - k_s)}{(k_s + 2k_f) - 2\phi(k_f - k_s)}, \quad Re = \frac{Ua}{v_f} \\ Ha &= \frac{\sigma_w \beta_0^2 a^2}{\mu_f} \end{aligned} \right\} \tag{16}$$

The dimensionless governing equations with an appropriate initial and boundary conditions can be written as:

$$\frac{\partial W}{\partial \bar{t}} = \frac{A}{Re(1 - \phi + \phi \rho_s / \rho_f)} + \frac{1}{Re(1 - \phi + \phi \rho_s / \rho_f)(1 - \phi)^{2.5}} \frac{\partial^2 W}{\partial \eta^2} - \frac{Ha}{Re} W \tag{17}$$

$$\frac{\partial \theta}{\partial \bar{t}} = \frac{1}{m Pr Re(1 - \phi + \phi \tau)} \frac{\partial^2 \theta}{\partial \eta^2} + \frac{Ec}{Re(1 - \phi + \phi \tau)(1 - \phi)^{2.5}} \left(\frac{\partial W}{\partial \eta} \right)^2 \tag{18}$$

The initial and boundary conditions for equations (18) and (19) are:

$$W(\eta, 0) = \theta(\eta, 0) = 0$$

$$W(0, \bar{t}) = \theta(0, \bar{t}) = 0 \tag{19}$$

$$W(1, \bar{t}) = 1, \quad \frac{\partial \theta}{\partial \eta}(1, \bar{t}) = -m Bi \theta(1, \bar{t})$$

Where Bi is the Biot number, Pr is the Prandtl number, Ec is the Eckert number and A is the pressure gradient parameter.

3 Entropy analysis

In analysis of entropy generation it is essential to diagnose the second law of thermo-dynamic which gives the base to analysis of effects of irreversibility caused by the nature of flow and heat transfer. The flow of nanofluids under convective cooling is incapable of being changed due the exchange of energy and momentum, within the nanofluid and at flow boundaries. According to Wood (1975) the volumetric rate of entropy generation is given by:

$$S''' = \frac{k_{nf}}{T_w^2} \left(\frac{\partial T}{\partial y} \right)^2 + \frac{\mu_{nf}}{T_w} \left(\frac{\partial u}{\partial y} \right)^2 \quad (20)$$

The partial differential equation (20) has two parts which are entropy generation due to heat transfer that is $\frac{k_{nf}}{T_w^2} \left(\frac{\partial T}{\partial y} \right)^2$ and entropy generation due to nanofluid friction represented by $\frac{\mu_{nf}}{T_w} \left(\frac{\partial u}{\partial y} \right)^2$.

Using dimensionless the equation (20) can be discretized as follows;

$$\Rightarrow \frac{a^2 S'''}{k_f} = \frac{1}{m} \left(\frac{\partial \theta}{\partial \eta} \right)^2 + \frac{Br}{(1-\phi)^2} \left(\frac{\partial W}{\partial \eta} \right)^2$$

Where

$$Ns = \frac{a^2 S'''}{k_f}, \quad N_1 = \frac{1}{m} \left(\frac{\partial \theta}{\partial \eta} \right)^2 \quad \text{and} \quad N_2 = \frac{Br}{(1-\phi)^2} \left(\frac{\partial W}{\partial \eta} \right)^2$$

From the discretized Partial differential equations we have entropy generation due to heat transfer and entropy generation due to nanofluid friction represented by N_1 & N_2 respectively.

Observing Equations (1)–(20), we can observe that they are inform of partial differential equations with given initial and boundary conditions. Equations (18)–(20) will be transformed to ordinary differential equations so that they can be easily solved using Runge–Kutta Fehlberg integration technique (Na 1979) and implemented on computer using Matlab software.

4 Numerical procedures

Using a discretization finite difference method the nonlinear initial boundary value problem (IBVP) in Equations (18)–(20) can be solved numerically. We partition the spatial interval $0 \leq \eta \leq 2$ into N equal parts and define the grid size $\Delta \eta = \frac{1}{N}$ and the grid points $\eta_i = (i-1)\Delta \eta$ and $1 \leq i \leq N+1$. The first and second partial differential equations were discretized using the central difference method. Let $W_i(t)$ and $\theta_i(t)$ be the approximation of $W(\eta_i, t)$ and $\theta(\eta_i, t)$ then the semi-discrete system for the problem becomes

$$\frac{dW_i}{d\bar{t}} = \frac{A}{Re(1-\phi + \phi \rho_s / \rho_f)} + \frac{W_{i+1} - 2W_i + W_{i-1}}{Re(1-\phi + \phi \rho_s / \rho_f)(1-\phi)^{2.5}(\Delta \eta)^2} - \frac{Ha}{Re} W_i \quad (21)$$

$$\frac{d\theta_i}{d\bar{t}} = \frac{\theta_{i+1} - 2\theta_i + \theta_{i-1}}{mPr Re(1-\phi + \phi \tau)(\Delta \eta)^2} + \frac{Ec}{Re(1-\phi + \phi \tau)(1-\phi)^{2.5}} \left(\frac{W_{i+1} - W_{i-1}}{2\Delta \eta} \right)^2 \quad (22)$$

With initial condition and boundary conditions

$$W_i(0) = \theta_i(0) = 0, \quad 1 \leq i \leq N+1, \quad W_1 = 0, \quad \theta_1 = 0, \quad W_{i+1} = 1, \quad \theta_{i+1} = (1 - mBi\Delta \eta), \quad W_i = \frac{fW_{i+1}}{f - \Delta \eta}$$

5 Results and Discussions

For understanding the dynamics of the designed model as shown in the figure 5, the intensively discussion for the problem has been discussed with great focus on velocity profiles, temperature profiles, effect of variation of parameters in different profiles and entropy generation. The dynamics and the observation of the results have been discussed as follows;

5.1 Effects of parameter variation on velocity profiles

From the figure 4 the observation shows that having different parameters it has proved that the Alumina-water nanofluid tends to flow faster than Copper –water nanofluid due to the fact that there is the great difference particularly in specific heat capacity. Also the observation shows that the change in space is negligible at the lower plate while experiencing small changes in space with increase in time. The observation shows that the space for the flow is significant immediately after $t=0.09$, while at $t<0.09$ the space for the flow is insignificant even though the time is increasing. Observing the figure

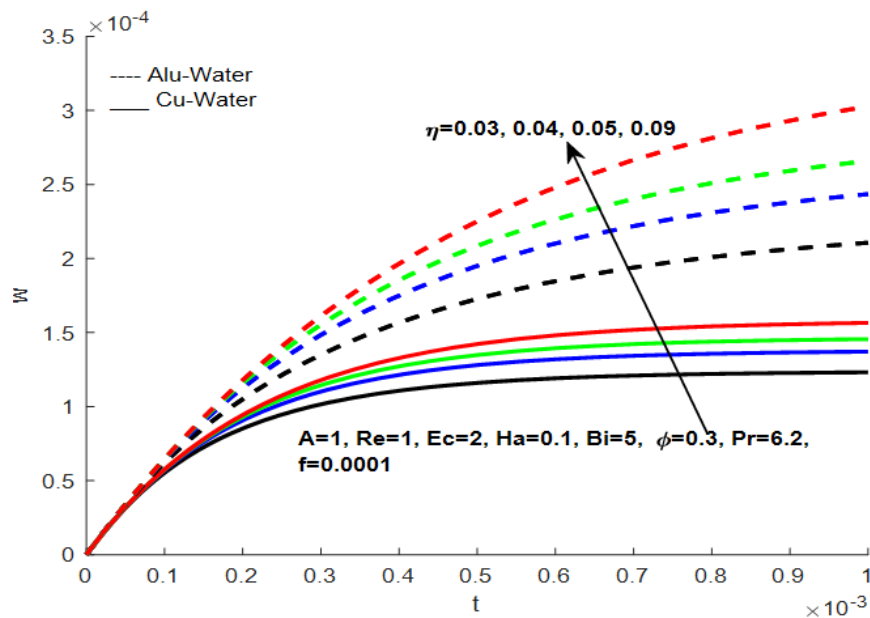


Fig. 6: Nanofluids velocity profile with profiles with increasing time.

6 the results shows that as space increases the velocity also increases but there is constant velocity from $\eta = 0$, up to $\eta = 0.9$ where the change in space has great significant for the lower plate to the upper plate. Also the observation shows that Alumina-water nanofluid tends to raise the velocity profile faster than copper-water due to the fact that copper has high density compared to Alumina. In a nutshell the nanoparticles bring effect at a very small space with a very small change in time as shown in the figure 7. From the figure 8 it is observed that as the space of the channel increases the velocity increases but there is no change in velocity at $\eta = 0$ up to $\eta = 0.093$, more interesting immediately at $\eta = 0.095$ the motion of the flow starts to rise. This may be due to the Navier Slip of the lower plate. Legibly it is observed that the increase of nanoparticles ϕ leads to the change of velocity of the channel from the lower plate towards the upper plate. Variation in nanoparticles ϕ has brought great results where at $\phi = 0$ shows that there is no mixture of nanoparticles rather it is purely water, but the nature of the flow changes soon after the increase of nanoparticles from $\phi = 0.1$ up to the maximum $\phi = 0.3$. From the figure 9 the result shows that with constant $\phi = 0.3$ and $\eta = 0.03$ the velocity increases as time increases. More

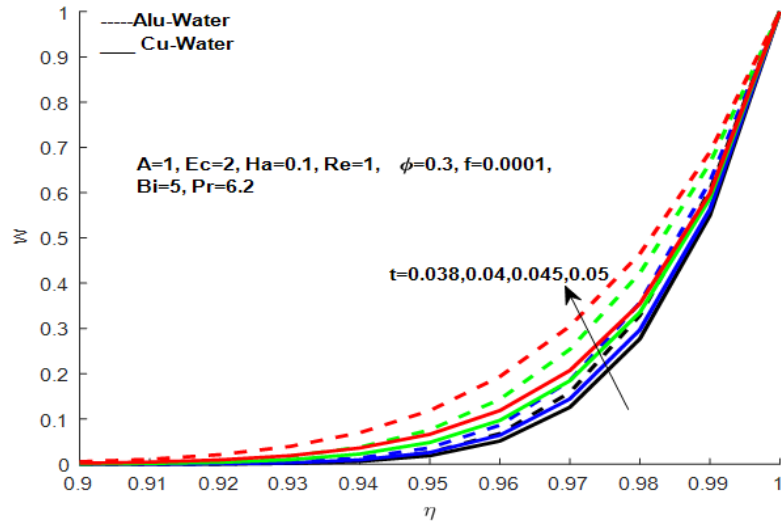


Fig. 7: Nanofluids velocity profile with profiles with increasing space.

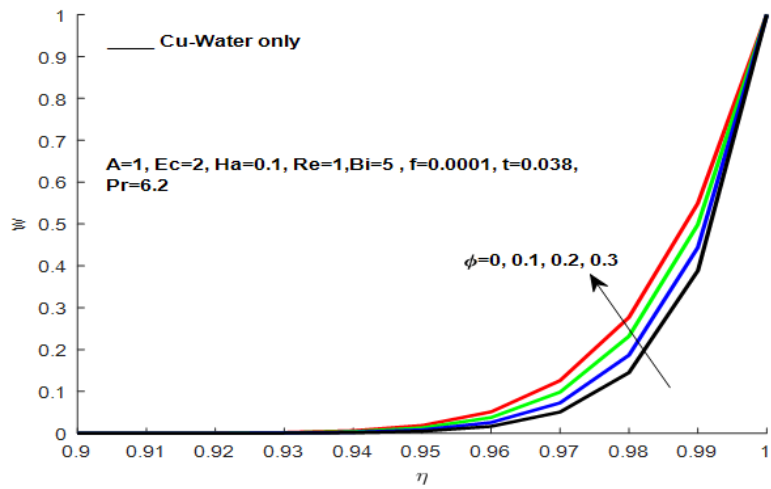


Fig. 8: Nanofluids velocity profile with increasing ϕ .

interesting the observation shows that as Reynolds increases the velocity of the profile increases. It was observed that as you increase Reynolds number, the velocity increases towards the upper plate but after $t = 1$ there is constant velocity as shown in the figure below. Observing the results shown in the figure 10 it is evidently that the velocity increases with increase in time. The increase of nanoparticles ϕ tends to raise the velocity of the profile. In other words the observation reveals that the higher the space the insignificant the velocity and the smaller the space the significant the velocity profile.

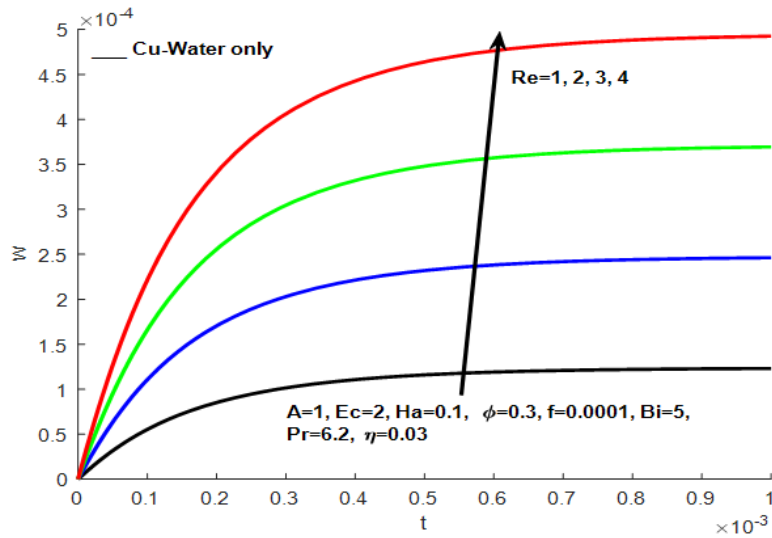


Fig. 9: Nanofluids velocity profile with increasing Re .

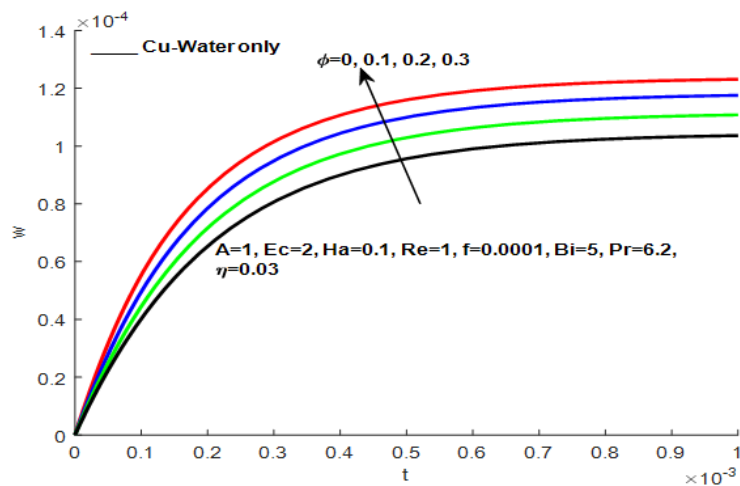


Fig. 10: Nanofluids velocity profile with increasing time (increasing ϕ).

5.2 Effects of parameter variation on temperature profiles

The result from the figure 11 shows that the temperature profile tends to increase with increase in time. Also the velocity increases with increase in space. Copper-water nanofluid tends to raise the temperature very faster than Alumina-water nanofluid; this may be due to their difference in specific heat capacity. The profile behaves with constant temperature immediately after $t = 1.6$. In a nutshell the change of temperature for both Alumina-water nanofluid and Copper-water nanofluid is more significant when the space is very larger and insignificant where the space is very smaller. The figure 12 describes the results of temperature variation profiles with combined nanofluids Alumina-water and Copper-water. The result shows that the temperature increases with the increase in space. Point to note is that the temperature profile behaves with constant temperature from lower plate to the upper plate but immediately after $\eta = 0.45$ the temperature profile rises very faster. Also the observation shows that Copper-water nanofluid tends to raise the temperature profile very fast than

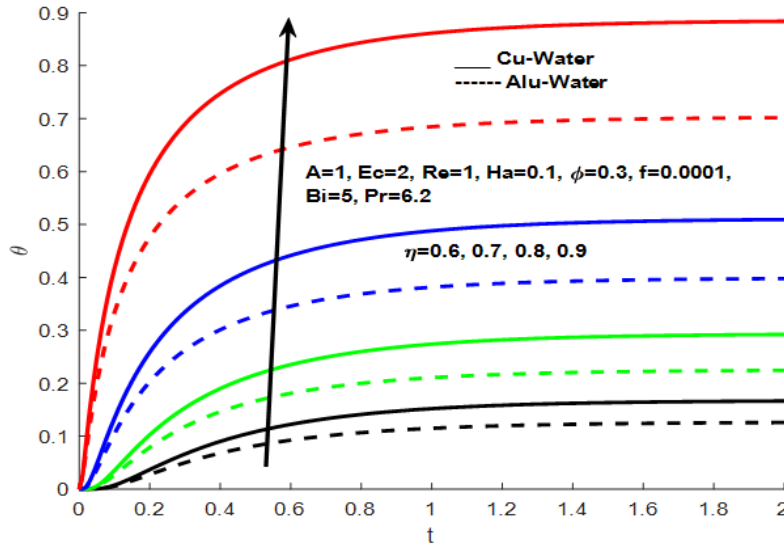


Fig. 11: Nanofluids temperature profile with profiles with increasing time.

Alumina-water nanofluid, this may be due to their differences in specific heat capacity and density. Observing the figure

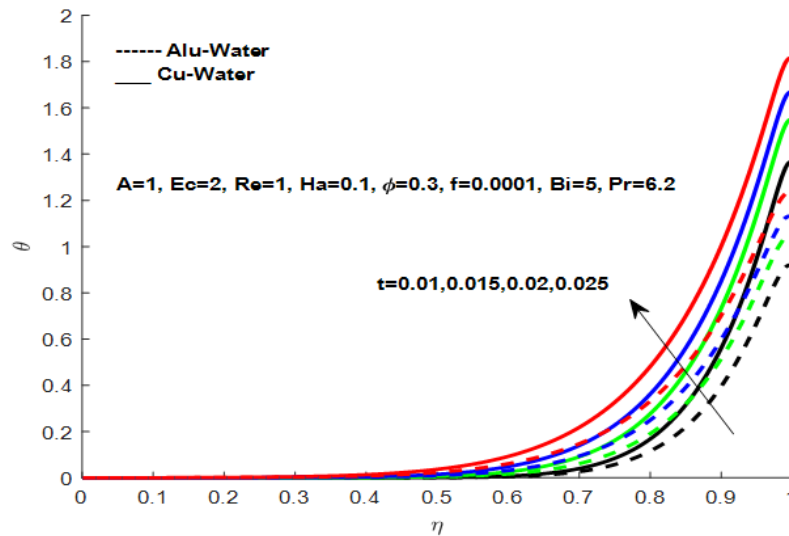


Fig. 12: Nanofluids temperature profile with increasing space.

13, the result show that the temperature increases with the increase in space but the temperature is constant in the lower plate from $\eta = 0$ up to $\eta = 0.5$, but soon after reaching $\eta = 0.58$ the temperature increases. Also the observation shows that the increase in Eckert number leads to the decrease in Temperature. This increase or decrease in temperature profile may be caused by viscous dissipation. In nutshell, the observation shows that as the Ec number increases the space also decreases with constant nanoparticles $\phi = 0.3$ and nanofluid fraction $f=0.0001$. From the figure 14 the result shows that the temperature increases with increase in space. The temperature profile in the lower plate the profile behaves with no

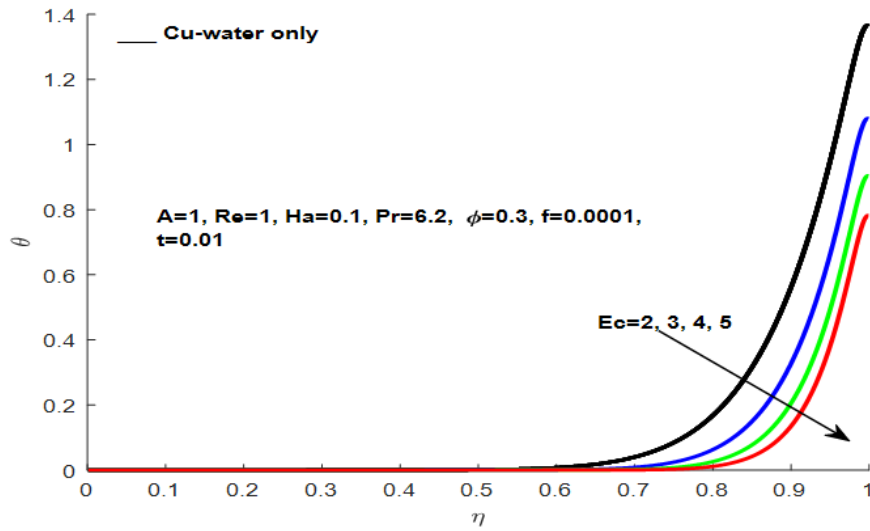


Fig. 13: Nanofluid temperature Profile with increasing Ec .

change in temperature but soon after reaching $\eta = 0.6$ the temperature rises very fast. With constant time $t=0.01$ and nanofluid fraction $f=0.0001$ the increase in nanoparticles $\phi = 0, 0.1, 0.2, 0.3$ lead to the increase in temperature under the fact that, the Navier slip in the lower plate there is no change of motion of the flow while when moving closer to the upper plate the temperature profile changes. The results in the figure 15 show that the temperature profile increases

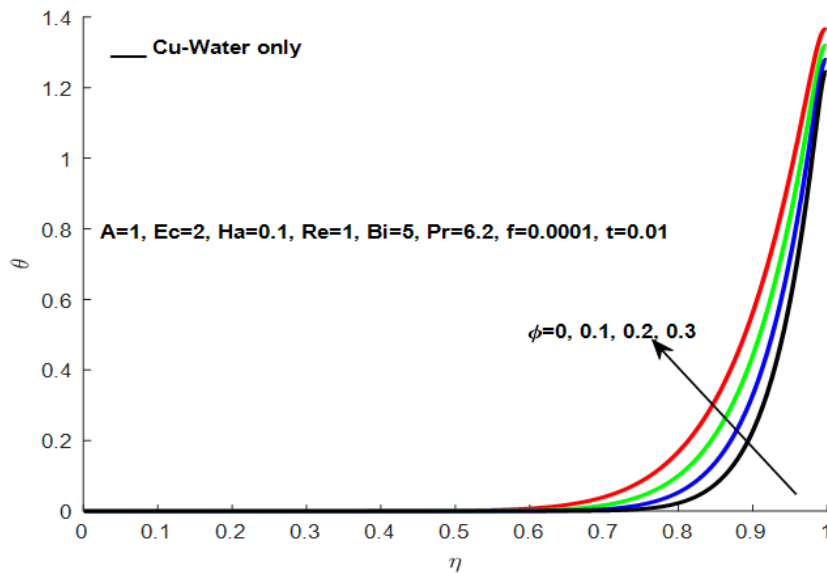


Fig. 14: Nanofluid temperature Profile with increasing ϕ .

with the increase in time but the point to note is that even though there is an increase in time the temperature is constant especially when the Eckert number increases. Also the observation shows that the increase in Eckert number leads to the

decrease in Temperature. This increase or decrease in temperature profile may be caused by the nature of the channel flow and the boundary of the flow (viscous dissipation). Further, the observation shows that as the Ec number increases the space also decreases with constant nanoparticles $\phi = 0.3$ and nanofluid fraction $f=0.0001$.

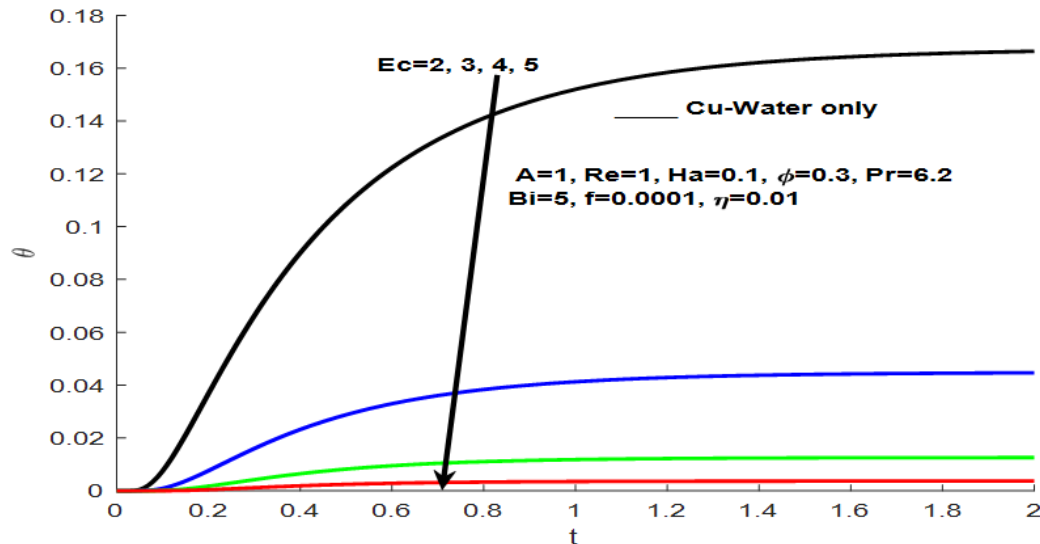


Fig. 15: Nanofluid temperature Profile with increasing Ec .

5.3 Effects of parameter on entropy generation

Considering the results shown in the figure 16, it shows that the entropy generation increases with the increase in space. Also the observation shows that the entropy generation rate is significant when the time is very larger but it is evidently that when the time is very smaller the entropy generation rate is not significant. In a broader observation, the result shows that as nanoparticles increases the entropy generation rate in the space of the interval $0 \leq \eta \leq 0.958$ does not change and the entropy generation starts to raise immediately after $\eta = 0.96$ while when it comes closer to the upper plate the entropy generation rate tends to diminish. This implies that the effect of entropy growth rate is significant in the upper plate while in the lower plate the entropy growth rate is constant. Observing the figure 17, the results shows that as entropy generation rate increases with increase in space but the results show that there is no change of entropy generation in the space interval from $\eta = 0$ up to $\eta = 0.958$ but immediately after $\eta = 0.96$ the entropy generation rate rises faster and this may be due to the fact that the rise of entropy generation takes place in large space while in smaller space the rate of increase is negligible. Also it important to notice that with constant nanoparticles $\phi = 0.3$. Also the observation shows that the increase of Ec number leads to the increase in entropy generation rate particularly in upper plate and this may be due to the relationship between the flows' kinetic energy and the boundary layer of the channel.

6 Conclusions

Numerical investigation of entropy generation in unsteady MHD generalized Couette flow with convective cooling of nanofluids Copper (Cu) and Alumina (Al_2O_3) as nanoparticles is presented. Using a semi-discretization method together with Runge-Kutta integration method the problem is solved numerically. The following are the summary of the

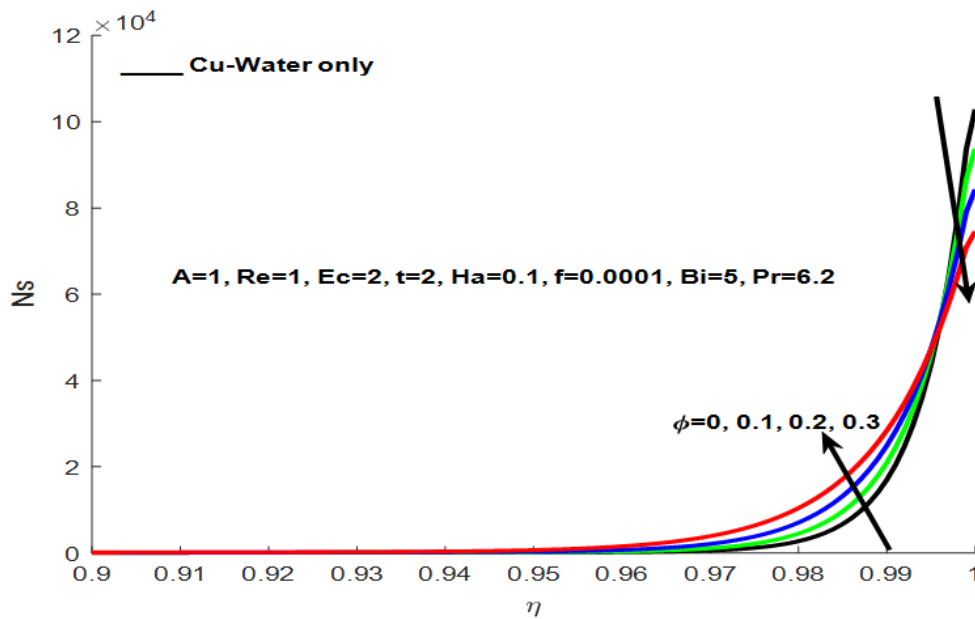


Fig. 16: Entropy generation rate with increasing ϕ .

obtained results.

An increase in nanoparticles and Reynolds number leads to increase in the velocity while pressure gradient, MHD and nanofluid fraction held constant. It is evidently that Alumina-water nanofluid tends to raise the velocity profile faster than Copper-water nanofluid. Also the results show that an increase in Eckert number causes the decrease in temperature profile. Further, it is noticed that Copper-water nanofluid tends to raise the temperature profile faster than Alumina-water nanofluid.

It is evidently that the entropy generation rises as the result of increase in Eckert number. Also it is noticed that entropy generation rises in lower plate but when it comes closer the upper plate the entropy generation rate starts to fall as the result of increase in nanoparticles.

Competing interests

The authors declare that they have no competing interests.

Authors' contributions

All authors have contributed to all parts of the article. All authors read and approved the final manuscript.

References

- [1] Ali A. O & Makinde O. D.(2015).Modelling the Effect of Variable Viscosity on Unsteady Couette Flow of Nanofluids with Convective Cooling. *Journal of Applied Fluid Mechanics*, Vol. 8, No. 4, pp. 793-802.

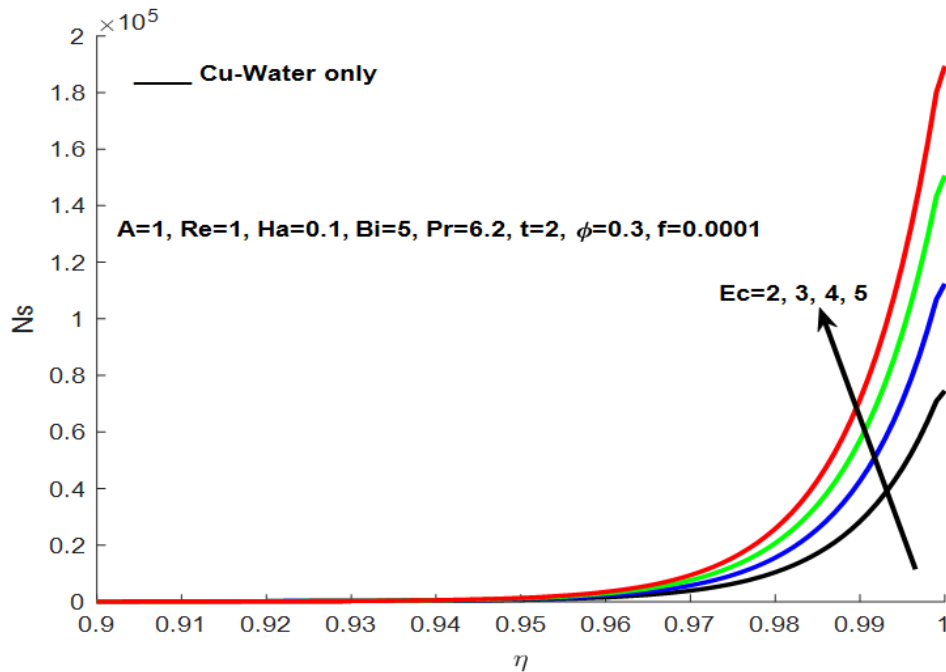


Fig. 17: Entropy generation rate with increasing Ec .

- [2] Bianco V., Nardini S. and Manca O. (2011). Enhancement of heat transfer and entropy generation analysis of nanofluids turbulent convection flow in square section tubes. *Nanoscale Research Letters*. 6 (1), pp 252.
- [3] Chen C., Chen B. and Liu C. (2014). Heat transfer and entropy generation in fully-developed mixed convection nanofluid flow in vertical channel. *International Journal of Heat and Mass Transfer*. 79, pp750-758.
- [4] E. Baskaya, G. Komurgoz and I. Ozkol (2017), "Investigation of Oriented Magnetic Field Effects on Entropy Generation in an Inclined Channel Filled with Ferrofluids". *International Journal of Pure and Applied Mathematics*, Vol.39, pp377.
- [5] Lyimo G.G & Mkwizu M. H. (2017). Numerical Investigation into Entropy Generation in a Channel Flow of Nanofluids with Convective Heating. Vol.4(1), pp 115-124.
- [6] Mkwizu M. H & Makinde O. D. (2014). Entropy generation in a variable viscosity channel flow of nanofluids with convective cooling. *Comptes Rendus Mecanique*. 343, pp38-56.
- [7] Mkwizu M. H., Makinde O. D and Nkansah-Gyekye Y. (2015). Second Law Analysis of Buoyancy Driven Unsteady Channel Flow of Nanofluids with Convective Cooling. *Applied and Computational Mathematics*, 4(1), pp 100-115
- [8] Mkwizu M. H., Makinde O. D & Nkansah-Gyekye Y. (2015). Numerical investigation into entropy generation in a transient generalized Couette flow of nanofluids with convective cooling. *SADHAWA-Indian Academic of Science*. 40, pp 2073 -2093.
- [9] Nur Husna MD Yusoff, MD., Jashim Uddin & Ahmad Izani MD. Ismail. Combined Similarity-numerical Solutions of MHD Boundary Layer Slip Flow of Non-Newtonian Power-law Nanofluids over a Radiating Moving Plate. 43(1), pp 151-159, 2014.
- [10] O.D. Makinde and A.S. Eegunjobi (2013). Analysis of Inherent Irreversibility in a Variable Viscosity MHD Generalized Couette Flow with Permeable Wall. *Journal of Thermal Science and Technology*. 8(1), pp 240-254.
- [11] O. D. Makinde and A. S. Eegunjobi, "Effects of convective heating on entropy generation rate in a channel with permeable walls," *Entropy*, vol.15, pp.220-233, 2013
- [12] Rashidi M. M., Abelman S. & Mehr N. F. (2013). Entropy generation in steady MHD flow due to a rotating porous disk in a nanofluid. *International Journal of Heat and Mass Transfer*. 62(2013), pp515-525.
- [13] S.O. Kareem, S.O. Adesanya, J.A. Falade and U.E. Vincent (2017). Entropy Generation Rate in Unsteady Buoyancy-driven Hydro-magnetic Couple Stress Fluid Flow Through a Porous Channel. *International Journal of Pure and Applied Mathematics*, vol 115, no. 2, pp.311-326, 2017.

- [14] T. Chinyoka and O. D. Makinde, “Unsteady hydro-magnetic flow of a reactive variable viscosity third-grade fluid in a channel with convective cooling,” *International Journal for Numerical Methods in Fluids*, vol.69,no.2, pp.353–365, 2012.